An active wearable dual-band antenna for GPS and Iridium satellite phone deployed in a rescue worker garment

Arnaut Dierck, Hendrik Rogier, Frederick Declercq
Electromagnetics Department
INTEC, Ghent University
Ghent, Belgium
arnaut.dierck@intec.ugent.be

***Abstract*—An active wearable dual-band circularly polarized microstrip patch antenna for Global Positioning System and Iridium satellite phone applications is presented. It is constructed using flexible foam and fabric substrates, combined with copper-on-polyimide film conductors. A low-noise amplifier chip is integrated directly underneath the antenna patch. The antenna's performance is examined under bending and on-body conditions. The active antenna gain is higher than 25 dBi and the 3dB axial ratio bandwidth exceeds 183 MHz in free-space conditions. The antenna performance is robust to bending and on-body placement.**

I. Introduction

Recently, wearable electronics have started to find their way into a growing amount of applications. Applying suitable materials, such as textiles and foams, enables unobtrusive integration of smart textile systems into garments, ranging from sports clothing to public service outfits [1]–[11]. A comfortable integration does, however, pose some design challenges in order to guarantee optimal antenna/electronics performance. Fabric/foam substrates introduce additional losses, and their flexibility, while required for conformal integration into clothing, makes the antennas vulnerable to bending, which might affect their performance. Also, proximity to the body and to other electronic devices must be taken into account.

To provide a highly reliable communications link in these conditions, miniaturization of the on-body electronic system is crucial. This approach produces less bulky electronic circuitry and antennas and improves wearability. The functionalities of different circuits/antennas are incorporated into more compact electronic units, reducing potential weak links between these devices. When looking at miniaturization from the antenna designer's perspective, it is thus desirable to replace multiple antennas by a single, broad band radiator. Electronics implementing the different functionalities serviced by this antenna can then also be centralized and their footprint size reduced. Accordingly, we have combined Global Positioning System (GPS) and Iridium satellite phone capabilities into one active antenna [2], integrating a low-noise amplifier (LNA) on the antenna feed plane.

Deploying the wearable antenna on a human body, together with additional adverse conditions, such as bending, crumpling and moisture absorption [12]–[16], causes the bandwidth and the resonant frequency to shift. Several circularly polarized wearable patch antennas for GPS and GPS/Iridium were already reported in literature [10], [17]–[19]. These antennas are based on topologies relying on asymetries in the patch to achieve circular polarization. This provides properly circularly polarized antennas, albeit in a limited frequency range, being insufficient to ensure an axial ratio < 3 dB in both GPS and Iridium bands.

In this contribution, an active wearable antenna is proposed that achieves circular polarization by means of a discrete hybrid coupler, providing an increased circular polarization bandwidth, covering both GPS and Iridium frequency bands. At the same time, it makes the antenna more robust to potential frequency shifts occuring when operating under adverse conditions or resulting from fabrication tolerances. The active part of the antenna consists of an LNA, amplifying the incoming signals to improve GPS and Iridium reception. For Iridium signal transmission, however, additional electronics would have to be included. The work from [11] has been extended with a field test, integrating the antenna in a firefighter jacket and connecting it to a portable GPS receiver. The antenna topology and the measures taken in order to achieve a robust wearable device are discussed in Section II. The antenna performance evaluation is documented in Section III.

II. Active Antenna Design and Topology

The active antenna is designed to meet the specifications for GPS L1 and Iridium reception. First, this requires coverage of the 2.046 MHz wide GPS L1-band, centered around 1.575 GHz, and the Iridium spectrum, ranging from 1.616 GHz to 1.6265 GHz [20]. Second, the antenna has to be right-handed circularly polarized in the above-mentioned frequency range. Furthermore, to facilitate integration into clothing, the antenna should be planar and low-profile. Antenna functionality has to be maintained under antenna bending conditions and in presence of the human body. To this aim, a microstrip patch antenna topology is selected, allowing easy integration into clothing, thanks to its low profile, and providing radiation away from the body in a semi-hemisphere. The

microstrip patch is aperture coupled through a dual-slotted ground plane to two perpendicular feed lines connected to an Anaren XC1400P-03S discrete quadrature hybrid coupler, providing a fixed 90° phase difference to provide circular polarization, as shown in Fig.1. The ground plane effectively shields the antenna patch from the active feed circuitry and from the human body. A hybrid coupler was preferred over other techniques, such as irregularities in the patch or feed geometry, to provide a broad band circular polarization, robust to fabrication tolerances and to frequency shifts caused by antenna bending. By preferring a discrete hybrid coupler over a microstrip realization, the footprint size is reduced, one the one hand, leaving place for the LNA chip to be integrated under the antenna patch, and, on the other hand, reducing the antenna's vulnerability to influences of antenna bending. The antenna geometry is symmetric with respect to the plane perpendicular to the xy-plane, forming a 45° angle with the x-axis. The wearablility of the antenna was ensured by applying flexible materials in the fabrication process. For the etched conductive surfaces, a laminate of 9 μm copper film on a 25 μm polyimide sheet was used. The antenna substrate consists of polyurethane foam (typically found in the shoulder pads of protective garments) with a thickness of 7.25 mm. This height was selected to provide wideband antenna performance, while maintaining a relatively simple feed structure, which is easy to fabricate and robust to bending conditions. For the feed substrate, aramid fabric (typically used as a an outer layer in protective garments) with a thickness of 400 μm is used. This layer is kept thin to minimize excess radiation from the feed circuit. The layers were assembled by means of thermally activated adhesive sheets. Table I lists the electromagnetic properties of the substrate materials. The active antenna contains a Maxim MAX2659 LNA chip [21], providing a high gain and a low noise figure. The layout of the LNA circuit is depicted in Fig. 2. Capacitor C_1 and inductor L_1 form the input matching network for the chip LNA, and capacitor C_2 provides decoupling of the supply voltage. The Anaren discrete hybrid coupler is, to the left, connected to the two perpendicular feeding arms, and, to the right, to the LNA input on the one port, and a 50 Ω termination (resistor R_1) on the other port. A low-profile UFL connector provides the interface between the LNA output and the receiving equipment. The antenna was modelled and optimized using ADS Momentum. The final dimensions are given in Table II. A photograph of the fabricated antenna is depicted in Fig. 3. The completed antenna structure measures 10.5 by 10.5 cm. The stacked foam/fabric/conductor layers have a total height of 7.6 mm. The electronic componenents don't add a lot of height, except for the discrete hybrid coupler, which has a height of 2.72 mm.

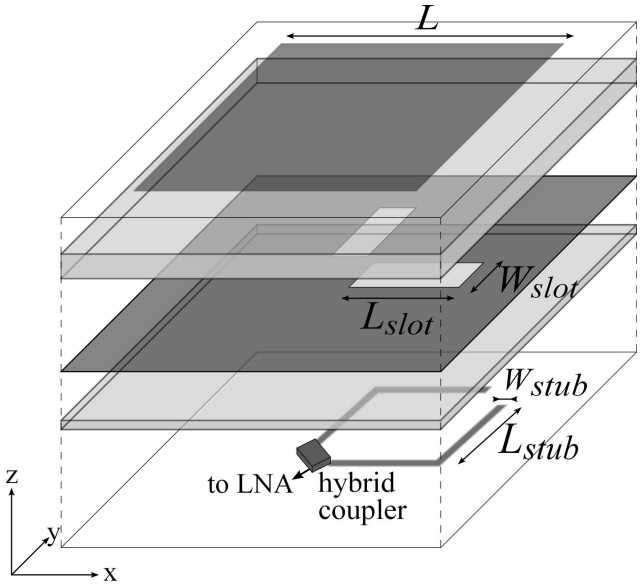

Fig. 1. Wearable GPS/Iridium active antenna topology

TABLE I
ELECTROMAGNETIC PROPERTIES OF THE ACTIVE ANTENNA MATERIALS

	ϵ_r	TAN δ	MATERIALS
Antenna substrate h_1=*7.25 mm*	1.25	0.02	polyurethane foam
LNA substrate h_2=*450 μm*	1.775	0.02	aramid textile fabric + polyimide layer

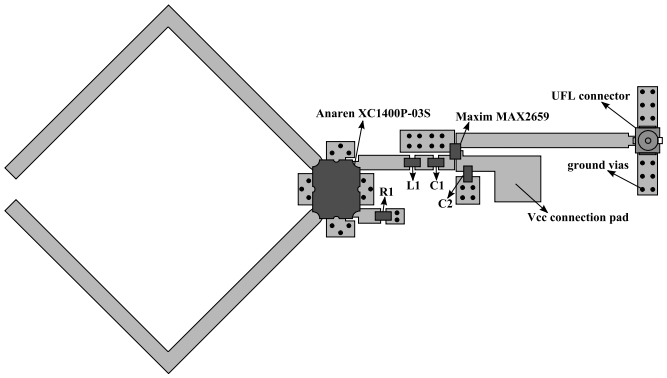

Fig. 2. Layout of LNA with chip amplifier

TABLE II
ANTENNA DIMENSIONS

Parameter	Value [mm]
L	70.85
L_{slot}	30
W_{slot}	5
L_{stub}	18
W_{stub}	1.62

III. ANTENNA PERFORMANCE EVALUATION

A. Anechoic chamber antenna characterization

The antenna performance was measured in an anechoic chamber by means of an Agilent N5241A PNA-X Vector Network Analyzer. First, conventional free-space antenna measurements were performed, without influence of bending and/or body proximity. Second, the antenna performance was measured while subjecting the antenna to bending in free-space, attaching it to a plastic cylinder with a 5 cm radius

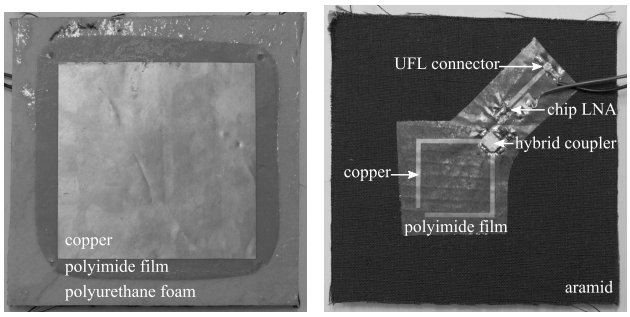

(a) (b)

Fig. 3. Photograph of active antenna prototype top (a) and bottom (b)

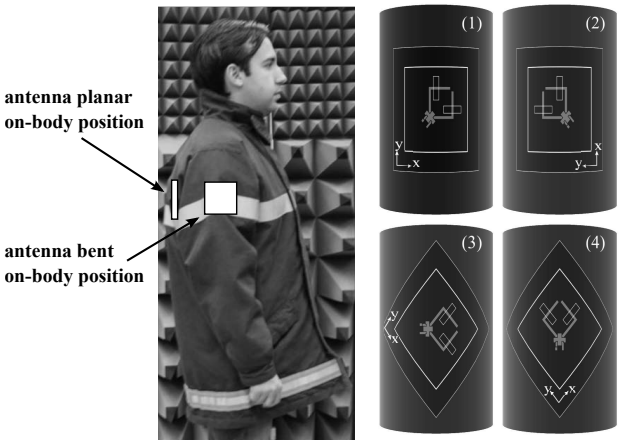

(a) (b)

Fig. 4. (a) Position of the antenna integrated in the firefighter jacket ; (b) Different bending directions of the antenna ((1) along the x-axis; (2) along the y-axis; (3) along the $y + 45°$-axis; (4) along the $y - 45°$-axis)

of curvature. Third, on-body measurements were carried out while the antenna was integrated in the rear section as well as in the upper part of the sleeve of a rescue worker jacket, behind the outer shell fabric and the combined thermal/moisture barrier, as depicted in Fig. 4(a). The rear section and sleeve positions allow the evaluation of the on-body antenna performance in planar and bent state, respectively. In order to characterize the effect of antenna bending, measurements were performed, both on- and off-body, in which the antenna was bent along the four directions displayed in Fig. 4(b): along the x-axis, y-axis, and $y \pm 45°$ axes. The circumference of the upper arm is 20 cm, corresponding to a radius of 3.2 cm. The jacket was worn by a male of average height and weight.

The free-space radiation pattern of the active receive antenna at 1.6 GHz is depicted in Fig. 5. The main beam gain equals 25.53 dBi. The antenna has a 3 dB beam width of 68°. The front-to-back ratio is 15 dB. The $|S_{11}|$ measured in free-space and on-body conditions, in both planar and bent state, is depicted in Fig. 6. The $|S_{11}|$ in free-space is lower than -10 dB from 1.36 GHz to 1.7 GHz, resulting in a matching bandwidth of 340 MHz. Bringing the antenna in the proximity of the body and subjecting it to different bending conditions does not substantially change this matching bandwidth. The hybrid coupler and LNA provide a robust, broad band 50 Ω match. The measured antenna gain is depicted in Fig. 7. The free space active antenna gain reaches a maximum of 25.43 dBi at 1.625 GHz. It stays within 1 dB of its maximum value from 1.558 to 1.677 GHz, a frequency range of 119 MHz. This frequency range is not significantly altered by the different measurement conditions. However, when exposing the antenna to bending and on-body conditions, the maximum gain changes and its corresponding frequency shifts. The most significant change occurs when the antenna is bent around the arm along the y-direction. Since there is no S-parameter data available on the LNA manufacturer's website, no simulation data have been included in Fig. 6 and 7. In Fig. 8, the measured axial ratio of the active antenna in free-space, on-body and bent positions is plotted as a function of frequency. The simulated free-space axial ratio results from exciting the radiating structure with 90° shifted input signals in ADS Momentum. For the free-space case, the measured axial ratio is lower than 3 dB from 1.517 GHz past the upper measurement frequency of 1.7 GHz, resulting in a 3 dB axial ratio bandwidth of over 183 MHz. The measured axial ratio is slightly higher than the simulated values, which can be explained by small shifts in the alignment of the different antenna layers during fabrication. When bending the antenna in a free-space setup, the axial ratio never exceeds 5 dB for the GPS and Iridium frequencies. It must be noted that this kind of bending represents a worst case scenario, which would only occur if the antenna was attached directly onto the human arm. When implemented in the lining of a jacket, the observed bending will be less severe. When deploying the antenna directly on the human body without bending, the axial ratio shifts downwards, resulting in a 3 dB axial ratio bandwidth larger than 200 MHz. When placing the antenna on a human arm, so that it is subjected to both body presence and bending, the axial ratio remains below 3 dB for two out of the four bending directions. In terms of on-body axial ratio performance, it is optimal to place this antenna in such a way that bending occurs along the x or $y + 45°$-axis.

B. Field test antenna evaluation

To verify the active antenna performance in a more realistic scenario, a GPS receiver was connected to the antenna, integrated in the upper sleeve of the firefighter jacket. The test person that previously had worn the firefighter jacket in the anechoic chamber measurements, now wore the jacket outside. The receiver was connected to a portable computer to monitor the results. This procedure was also carried out with an off-the-shelf rigid active antenna, provided with the receiver, for use as a reference scenario. Both antennas were tested in short succession, to minimize the influence of changes in the satellite constellation on the received signals. The active wearable antenna and the off-the-shelf rigid active antenna both had 9 satellites in view, of which they were able to use 7 to perform localization. The average carrier-to-receiver noise density when using the wearable active antenna and the off-the-shelf active antenna was 39.5 and 35.5 dB-Hz,

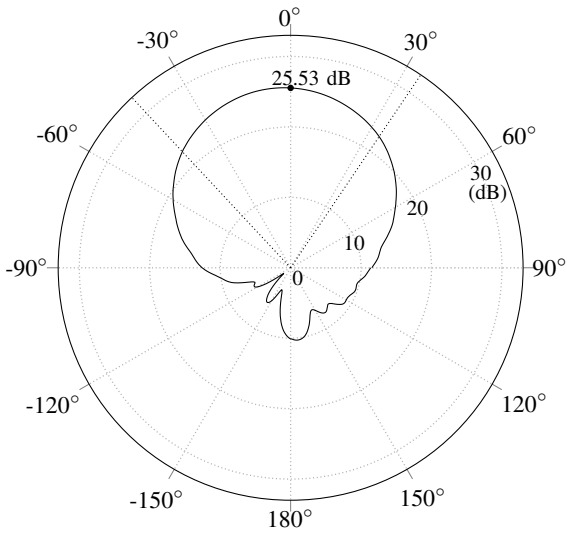

Fig. 5. Radiation pattern of the active wearable antenna at 1.6 GHz in the xz-plane

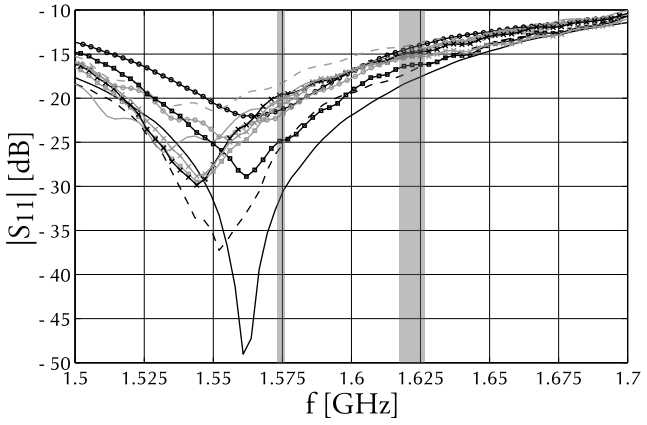

Fig. 6. Measured $|S_{11}|$ of active antenna (— planar; - - on-body; -o- bent x; — bent y; - - bent $y + 45°$; -o- bent $y - 45°$; -□- arm x; -□- arm y; -×- arm $y + 45°$; -×- arm $y - 45°$)

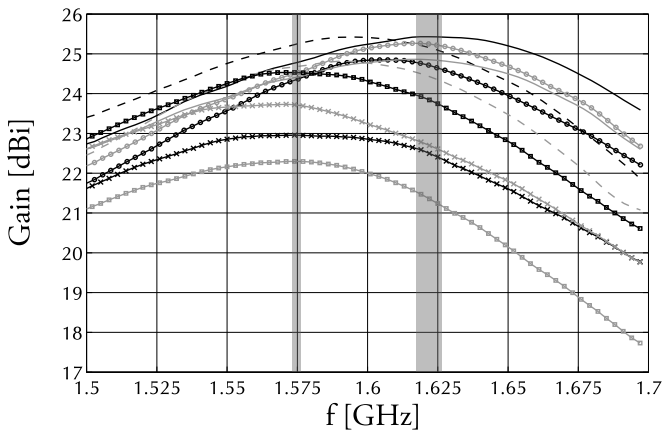

Fig. 7. Measured gain of active antenna (— planar; - - on-body; -o- bent x; — bent y; - - bent $y + 45°$; -o- bent $y - 45°$; -□- arm x; -□- arm y; -×- arm $y + 45°$; -×- arm $y - 45°$)

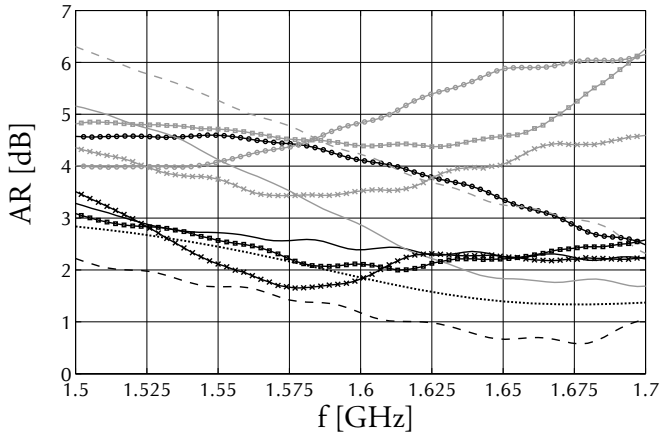

Fig. 8. Simulated (···) and measured axial ratio of active antenna (— planar; - - on-body; -o- bent x; — bent y; - - bent $y + 45°$; -o- bent $y - 45°$; -□- arm x; -□- arm y; -×- arm $y + 45°$; -×- arm $y - 45°$)

demonstrating that the wearable active antenna exhibits a performance that is comparable to the rigid alternative.

IV. CONCLUSION

In this contribuition, the design of a combined GPS/Iridium wearable active antenna was discussed. Flexible, wearable materials were used to construct the active antenna which has an LNA integrated onto its feed plane. The antenna is robustly matched over a wide frequency range under bending and on-body conditions. The discrete hybrid coupler provides circularly polarized behavior over a broad frequency range. The antenna has a free-space gain that exceeds 25 dBi. Circular polarization is ensured in a wide frequency range starting at 1.517 GHz and extending beyond 1.7 GHz in unbent state. The antenna's axial ratio remains lower than 5 dB for GPS and Iridium frequencies in all conditions, except when the antenna is bent along $y - 45°$, where the axial ratio exceeds 5 dB for Iridium frequencies. For the antenna placed on-body, the planar positions and the x and $y + 45°$ bending positions result in an axial ratio that remains lower than 3 dB. Each of these positions provides a sufficiently wide axial ratio bandwidth for proper GPS and Iridium reception. When connecting the active antenna, integrated in the sleeve of a firefighter jacket, to a commercial GPS receiver, it provides a performance that is comparable to a rigid off-the-shelf active antenna, having the same number of satellites in view and a higher average carrier-to-receiver noise density.

REFERENCES

[1] A. Dierck, T. De Keulenaer, F. Declercq, and H. Rogier, "A wearable active GPS antenna for application in smart textiles," in *Proc. of the 32nd ESA Antenna Workshop on Antennas for Space Applications*, Noordwijk, the Netherlands, oct. 2010.

[2] A. Dierck, F. Declercq, and H. Rogier, "Review of active textile antenna co-design and optimization strategies," in *2011 IEEE Int. Conference on RFID-Technologies and Applications (RFID-TA)*, sept. 2011, pp. 194 – 201.

[3] G. Orecchini, L. Yang, M. Tentzeris, and L. Roselli, ""Smart Shoe": An autonomous inkjet-printed RFID system scavenging walking energy," in *2011 IEEE Int. Symp. on Antennas and Propagation (APSURSI)*, july 2011, pp. 1417 –1420.

[4] B. Gupta, S. Sankaralingam, and S. Dhar, "Development of wearable and implantable antennas in the last decade: A review," in *2010 Mediterranean Microwave Symp. (MMS)*, aug. 2010, pp. 251 –267.

[5] L. Vallozzi, W. Vandendriessche, H. Rogier, C. Hertleer, and M. L. Scarpello, "Wearable textile gps antenna for integration in protective garments," in *2010 Proc. of the Fourth European Conference on Antennas and Propagation (EuCAP)*. IEEE, 2010, p. 4. [Online]. Available: http://galayaa.com/EUCAP/data/1841658.pdf

[6] L. Vallozzi, P. Van Torre, C. Hertleer, H. Rogier, M. Moeneclaey, and J. Verhaevert, "Wireless communication for firefighters using dual-polarized textile antennas integrated in their garment," *IEEE Trans. Antennas Propag.*, vol. 58, no. 4, pp. 1357–1368, 2010.

[7] L. Vallozzi, H. Rogier, and C. Hertleer, "Dual polarized textile patch antenna for integration into protective garments," *IEEE Antennas Wireless Propag. Lett.*, vol. 7, pp. 440–443, 2008.

[8] A. Tronquo, H. Rogier, C. Hertleer, and L. Van Langenhove, "Robust planar textile antenna for wireless body LANs operating in 2.45 GHz ISM band," *Electron. Lett.*, vol. 42, no. 3, pp. 142–143, 2006.

[9] T. Kennedy, P. Fink, A. Chu, N. Champagne, G. Lin, and M. Khayat, "Body-worn E-Textile antennas: The good, the low-mass, and the conformal," *IEEE Trans. Antennas Propag.*, vol. 57, no. 4, pp. 910–918, 2009.

[10] E. Kaivanto, M. Berg, E. Salonen, and P. de Maagt, "Wearable circularly polarized antenna for personal satellite communication and navigation," *IEEE Trans. Antennas Propag.*, vol. 59, no. 12, pp. 4490 –4496, dec. 2011.

[11] A. Dierck, H. Rogier, and F. Declercq, "A wearable active antenna for global positioning system and satellite phone," *IEEE Trans. Antennas Propag.*, vol. 61, no. 2, pp. 532–538, 2013.

[12] Q. Bai and R. Langley, "Crumpling of PIFA textile antenna," *IEEE Trans. Antennas Propag.*, vol. 60, no. 1, pp. 63 –70, Jan. 2012.

[13] P. Salonen and Y. Rahmat-Samii, "Textile antennas: Effects of antenna bending on input matching and impedance bandwidth," *IEEE Aerosp. Electron. Syst. Mag.*, vol. 22, no. 3, pp. 10–14, 2007.

[14] C. Hertleer, A. Van Laere, H. Rogier, and L. Van Langenhove, "Influence of relative humidity on textile antenna performance," *Textile Research J.*, vol. 80, no. 2, p. 177, 2010.

[15] C. Hertleer, A. Tronquo, H. Rogier, L. Vallozzi, and L. Van Langenhove, "Aperture-coupled patch antenna for integration into wearable textile systems," *IEEE Antennas Wireless Propag. Lett.*, vol. 6, pp. 392–395, 2007.

[16] P. Salonen, Y. Rahmat-Samii, and M. Kivikoski, "Wearable antennas in the vicinity of human body," in *2004 IEEE Antennas and Propagation Society Int. Symp.*, vol. 1. IEEE, 2004, pp. 467–470.

[17] I. Locher, M. Klemm, T. Kirstein, and G. Troster, "Design and Characterization of Purely Textile Patch Antennas," *IEEE Trans. Adv. Packag.*, vol. 29, no. 4, pp. 777 –788, nov. 2006.

[18] P. Salonen, Y. Rahmat-Samii, M. Schaffrath, and M. Kivikoski, "Effect of textile materials on wearable antenna performance: a case study of GPS antennas," in *2004 IEEE Antennas and Propagation Society Int. Symp.*, vol. 1, june 2004, pp. 459 – 462 Vol.1.

[19] L. Vallozzi, W. Vandendriessche, H. Rogier, C. Hertleer, and M. Scarpello, "Design of a protective garment GPS antenna," *Microwave and optical technology lett.*, vol. 51, no. 6, pp. 1504–1508, 2009.

[20] S. Pratt, R. Raines, C. Fossa, and M. Temple, "An operational and performance overview of the iridium low earth orbit satellite system," *IEEE Commun. Surveys Tuts.*, vol. 2, no. 2, pp. 2–10, 1999.

[21] Maxim Integrated Products, *GPS/GNSS Low Noise Amplifier, MAX2659 data sheet*, August 2011. [Online]. Available: http://datasheets.maxim-ic.com/en/ds/MAX2659.pdf